Supporting Information for "GRACE satellite observations of Antarctic Bottom Water transport variability"

Jemma Jeffree[1,2], Andrew McC. Hogg[1,2], Adele K. Morrison[1,2,3], Aviv Solodoch[4], Andrew L. Stewart[5], Rebecca McGirr[1,3]

[1]Research School of Earth Sciences, Australian National University, Canberra, ACT, Australia

[2]ARC Centre of Excellence for Climate Extremes, Australia

[3]The Australian Centre for Excellence in Antarctic Science, University of Tasmania, Hobart, Tasmania, Australia

[4]Institute of Earth Sciences, Hebrew University of Jerusalem, Jerusalem, Israel

[5]Department of Atmospheric and Oceanic Sciences, University of California, Los Angeles, CA 90095, USA

Contents of this file

1. Modification of density threshold in GFDL-OM4

We found that defining AABW according to maximum overturning in the Pacific Ocean in GFDL-OM4-025 lead to an unrealistic representation of AABW location and correspondingly poor reconstruction skill. The density threshold that maximises mean AABW transport in GFDL-OM4-025 is 1037.02 kg/m^3, but this shifts the AABW to include shallower depths than in ACCESS-OM2-01, and to include water in the eastern Pacific (Figures S1 a and b). Using the ACCESS-OM2-01 definition of AABW in GFDL-OM4-025 produces an estimate of AABW which is of similar volume and location to AABW in ACCESS-OM2-01. Observations suggest there is minimal net AABW transport in the east Pacific (Cimoli et al., 2023, Fig 5), supporting the use of a higher density threshold. The higher density threshold also improves the skill of AABW transport reconstructions (Figures S1 c and d).

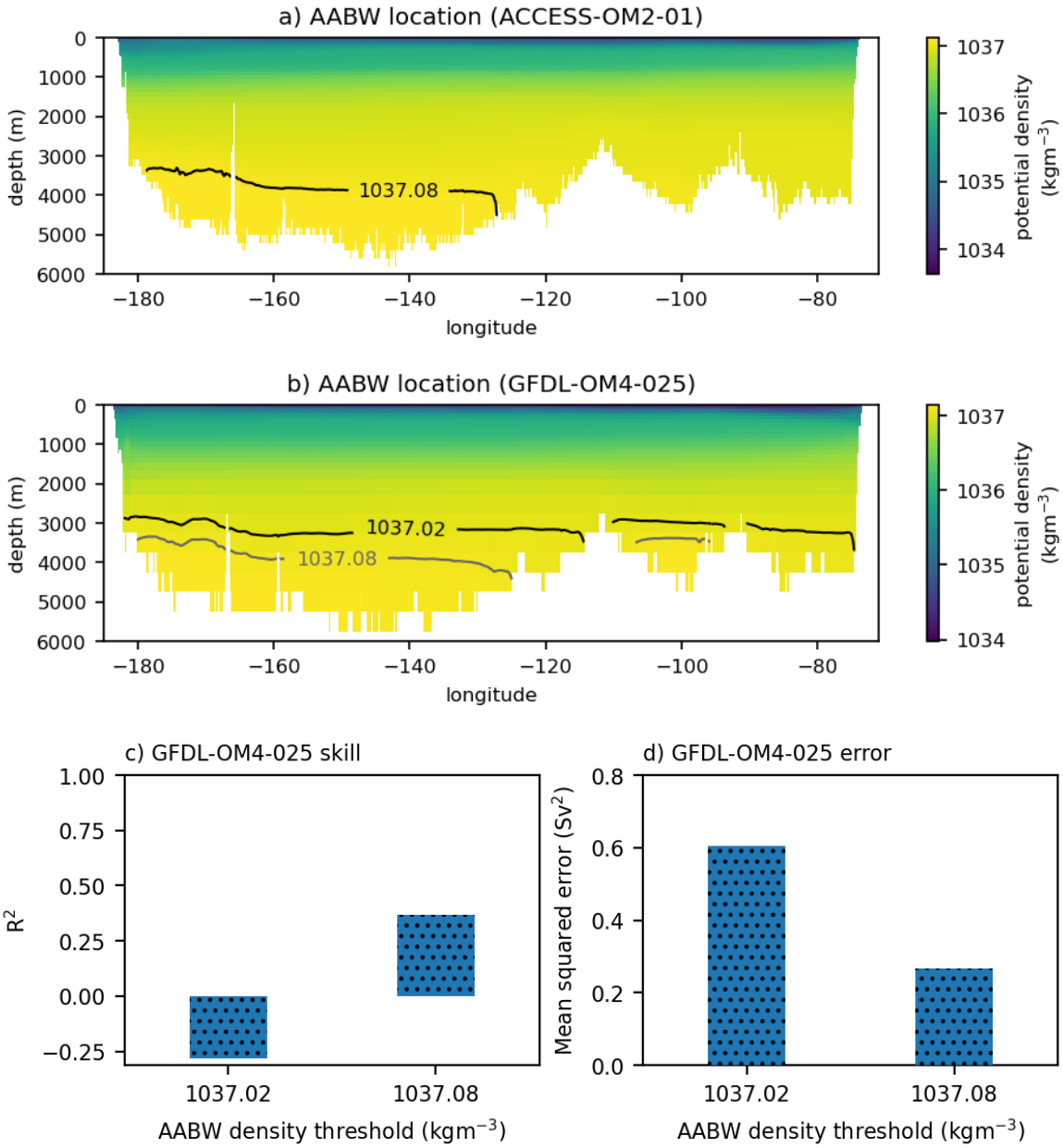

Figure S1. The influence of AABW density threshold in the Pacific Ocean on the physical location of AABW and reconstruction skill of AABW transport. a) ρ_2 potential density (colors) and the defining contour (in black) of of AABW in ACCESS-OM2-01 historically forced run, for reference. b) ρ_2 potential density (colors) and the defining contour (grey/black) of AABW in GFDL-OM4-025, defined using both the maximum overturning (1037.02 kg/m^3, black) and ACCESS-OM2-01 definition (1037.08 kg/m^3, grey). c) and d) show the R^2 and RMSE respectively for AABW transport reconstructions in GFDL-OM4-025, using each AABW definition.

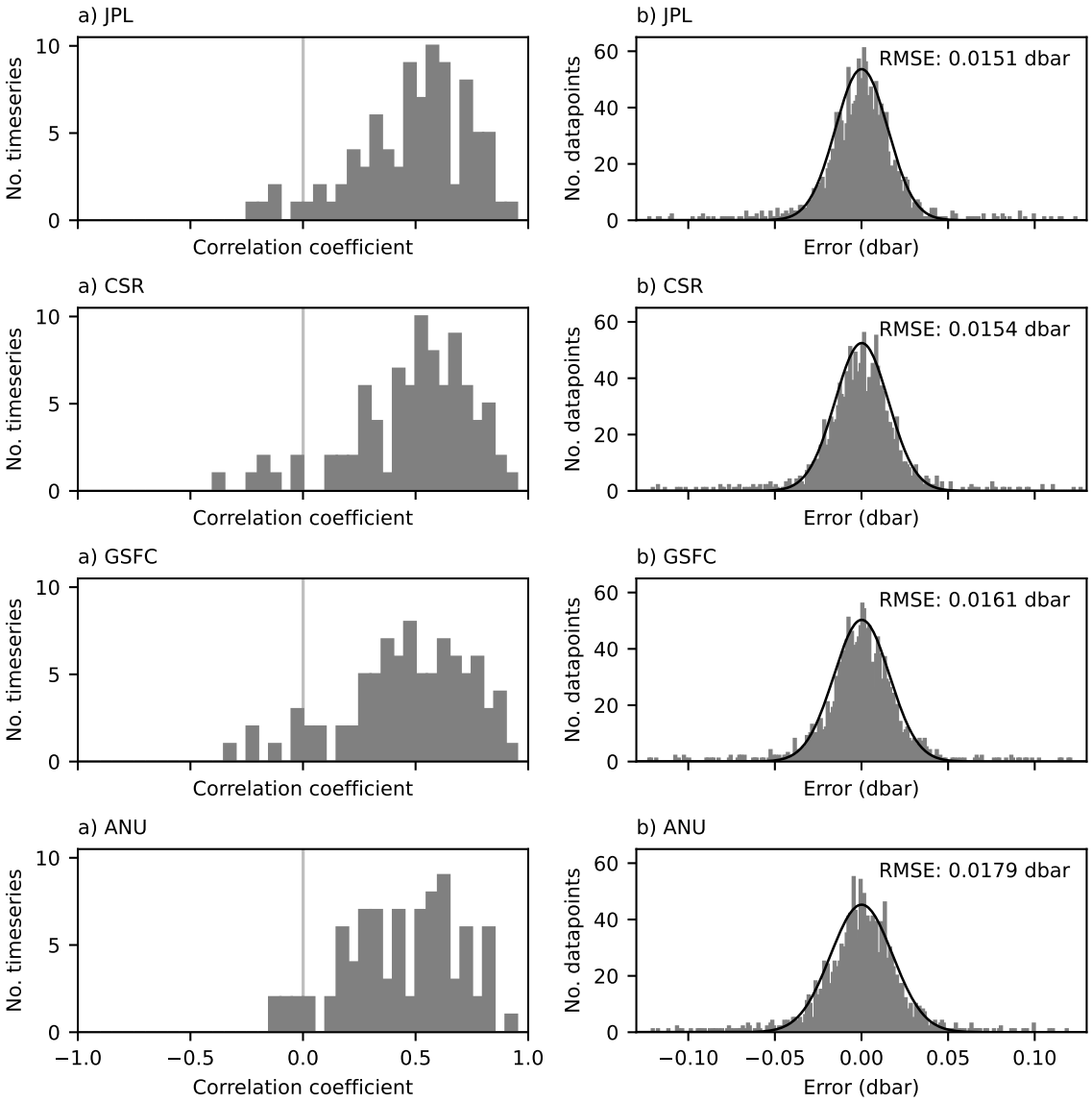

Figure S2. Empirical error estimation of four different GRACE products. The Jet Propulsion Laboratory (JPL) GRACE mascon product RL06mv3 (a,b) has lower RMSE than other products tested. c,d) Centre for Space Research (CSR) mascon product RL06.2 (Save et al., 2016; Save, 2020) e,f) Goddard Space Flight Centre (GSFC) mascon product RL06v2.0(Loomis et al., 2019) g,h) Australian National University solutions (ideally we'll have a ref sometime soon). All except the ANU solutions are taken from a regridded product.

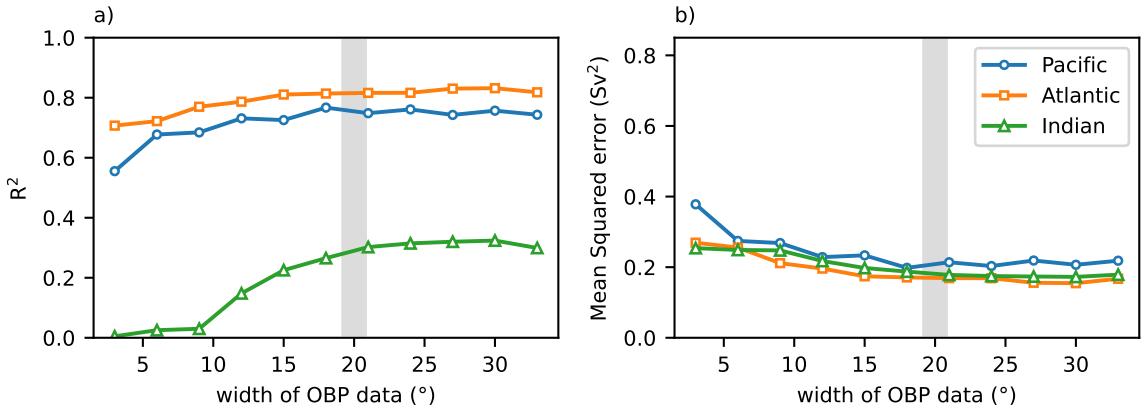

Figure S3. Influence of different latitude widths of ocean bottom pressure data used to reconstruct AABW transport on a) reconstruction skill and b) mean squared error. Grey shading indicates the width of latitude used in the rest of this work.

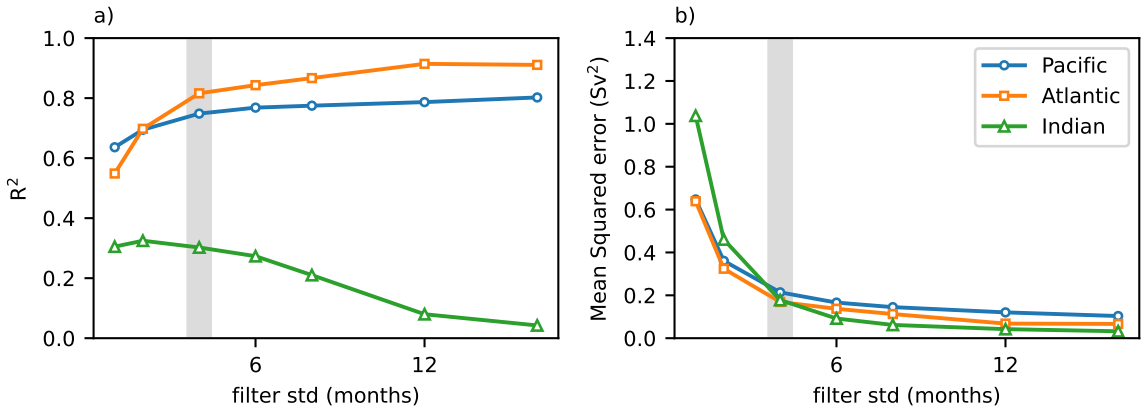

Figure S4. Influence of different temporal filtering length on a) reconstruction skill and b) mean squared error. Grey shading indicates the temporal filter used in the rest of this work.

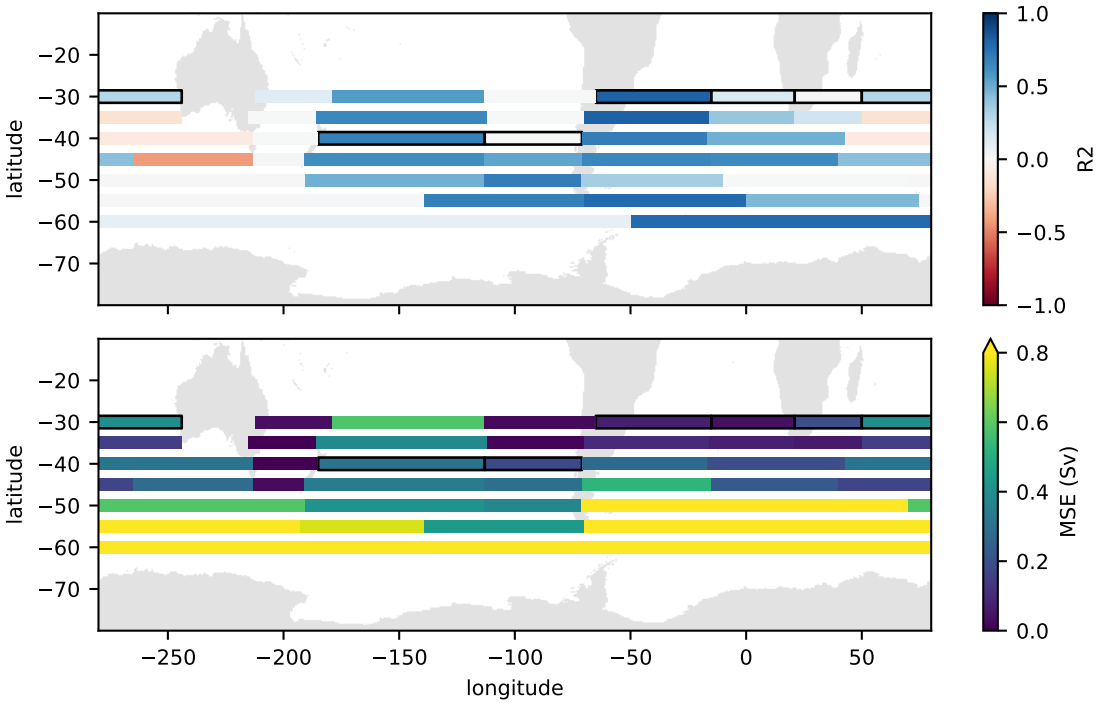

Figure S5. Influence of location at which transport is calculated on a) reconstruction skill and b) mean squared error. Black outlines indicate the transects used in the rest of this work.

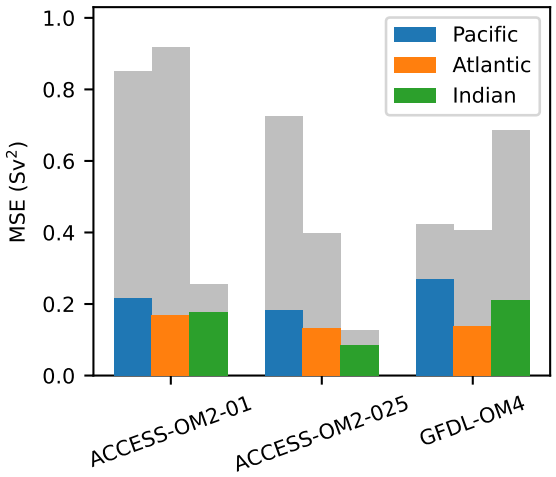

Figure S6. As per Figure 7b: MSE of AABW transport reconstruction in different models, but with grey shading indicating the total AABW variance after temporal smoothing, for comparison.

References

Cimoli, L., Gebbie, G., Purkey, S. G., & Smethie, W. M. (2023). Annually resolved propagation of CFCs and SF6 in the global ocean over eight decades. *Journal of Geophysical Research: Oceans*, *128*(3), e2022JC019337. Retrieved from https://agupubs.onlinelibrary.wiley.com/doi/abs/10.1029/2022JC019337 (e2022JC019337 2022JC019337) doi: https://doi.org/10.1029/2022JC019337

Loomis, B. D., Luthcke, S. B., & Sabaka, T. J. (2019). Regularization and error characterization of GRACE mascons. *Journal of Geodesy*, *93*(9), 1381–1398. Retrieved from https://doi.org/10.1007/s00190-019-01252-y doi: 10.1007/s00190-019-01252-y

Save, H. (2020). *Csr GRACE and GRACE-fo rl06 mascon solutions v02.* online. doi: doi: 10.15781/cgq9-nh24

Save, H., Bettadpur, S., & Tapley, B. D. (2016). High-resolution csr GRACE rl05 mascons. *Journal of Geophysical Research: Solid Earth*, *121*(10), 7547-7569. Retrieved from https://agupubs.onlinelibrary.wiley.com/doi/abs/10.1002/2016JB013007 doi: https://doi.org/10.1002/2016JB013007